Journal of Thermal Analysis and Calorimetry
https://doi.org/10.1007/s10973-024-13009-7

The influence of La and Ce additions on the solidification of alloys from the Al–Fe system

Maja Vončina[1] · Jožef Medved[1] · Matej Steinacher[2] · Klavdija Ozimič[2]

Received: 3 October 2023 / Accepted: 20 February 2024

Abstract
Aluminium alloys are popular in modern applications due to their lightweight, high strength and ductility. Alloys in the 8xxx series have similar properties to those in the 1xxx series, but are stronger, are more malleable and have higher stiffness. The addition of rare earths (RE) can refine the as-cast microstructure and, as a result, can increase the corrosion resistance and mechanical properties of aluminium alloys at room and high temperatures. The effects of rare earth (Ce and/or La) additions to Al-1.4Fe alloys were investigated. Thermal analysis of the solidification behaviour of the reference alloy showed the occurrence of three reactions corresponding to the formation of α-Al, eutectic (α-Al + Al_xFe_y) and Fe intermetallics, respectively. The results showed similar reactions for the Ce- and/or La-modified alloy, but at slightly different temperatures, indicating a change in the forming phases due to the addition of Ce and/or La. In all cases, the microstructures were typically hypoeutectic, consisting of the primary α-Al and the eutectic (α-Al + Al_xFe_y). The effect of grain refinement of the primary α-Al grains of the as-cast alloy was observed by the addition of RE, while La showed the strongest effect. The effect of the RE additions showed no obvious differences in the morphology of the eutectic Al_xFe_y, although they were present in these phases. When Ce and/or La were added, (α-Al + $Al_{11}Ce_3$) and/or (α-Al + $Al_{11}La_3$) eutectics were formed, while Fe was not detected in these eutectics.

Keywords Al–Fe alloys · Lanthanum and/or cerium addition · Solidification · Microstructure

Introduction

Aluminium alloys are popular in modern applications due to their lightweight, high strength and ductility. Alloys in the 8xxx series have similar properties to those in the 1xxx series but have higher strength, better formability and greater stiffness [1, 2]. Incorporating rare earth (RE) into aluminium alloys presents an opportunity to enhance their microstructure, corrosion resistance and mechanical properties, at both room temperature and elevated temperatures. The practice of RE micro-alloying is a prevalent technique in conventional casting methods for diverse aluminium alloys. Additionally, it facilitates the modulation of heterostructure growth by adjusting the composition of micro-alloyed atoms in the alloy [3]. Studies have shown the positive influence of RE elements on the properties of Al–Fe aluminium alloys [4–6].

Al–Fe alloys often exhibit coarse Al_xFe_y phases with feathery, plate-like or needle-like morphology, which can reduce ductility due to stress concentration [7]. Unfortunately, coarse Al_xFe_y phases such as Al_3Fe ($Al_{13}Fe_4$), Al_mFe or Al_6Fe usually form because the maximum solid solubility of Fe in Al is very low. To improve the strength properties of Al–Fe alloys, it is recommended to modify the microstructure using grain refiners, alloying elements or heat treatment modifications [8, 9]. AA8176 aluminium alloy, which has excellent electrical conductivity and high specific strength, has great potential for various applications [10]. Studies have shown that the addition of La-rich RE mixtures to Al–Fe alloys can refine the Al_3Fe eutectic phase and improve the microstructure and mechanical properties [3]. Small quantities of La contribute to the refinement of α-Al grains [11, 12] and the alteration of the $Al_{13}Fe_4$ intermetallic phase, resulting in heightened elongation and electrical

✉ Maja Vončina
maja.voncina@ntf.uni-lj.si

[1] Faculty of Natural Sciences and Engineering, Department for Materials and Metallurgy, University of Ljubljana, Aškerčeva 12, 1000 Ljubljana, Slovenia

[2] Impol, d. o. o., Partizanska Ulica 38, 2310 Slovenska Bistrica, Slovenia

Published online: 26 March 2024

conductivity. Nevertheless, an excessive La may induce the formation of the $A_{l1}1La_3$ phase, leading to a reduction in elongation [10, 12, 13].

An alternative rare earth (RE) addition to consider is Ce. As reported by Liang et al. [8], a combination of RE elements can efficiently refine both the α-Al grain and the intermetallic $A_{l3}Fe/Al_6Fe$ in an Al-2 mass % Fe alloy. With a 0.5 mass % RE addition, the average grain size of primary α-Al becomes half the size compared to the alloy without RE. The introduction of mixed RE initially enhances and subsequently diminishes the mechanical properties of the alloys. The RE elements that accumulate before the solid–liquid interface form Al_8Fe_2Ce at the grain boundaries of α-Al. The addition of 0.7 mass % mixed RE resulted in preferential formation of the granular $Al_{11}Ce_3$ in which La was dissolved. Nonetheless, the emergence of $Al_{11}Ce_3$ diminished the refining influence of the mixed RE combination, adversely affecting the mechanical properties of the alloy. Through uniform annealing, the lamellar Al_xFe_y phase is transformed into short rods, and subsequent cold rolling disperses the second phase, distributing it evenly within the primary α-Al matrix. The alloy, with a 0.5 mass % mixed RE addition, exhibits a remarkable improvement in elongation and tensile strength—50.14% and 10.67% higher, respectively—compared to the unmodified alloy in the cold-rolled state [8].

Some researchers also reported that the addition of La and Ce elements to aluminium alloys can remove harmful impurities such as Fe and Si, refine grain size, change microstructure and improve inclusion phase distribution and electrical conductivity [14]. A Ce content of 0.05–0.16 mass % in Al rods has a particularly positive effect on electrical conductivity and tensile strength, as it reduces the solid solubility of impurities in the aluminium matrix [15–17]. Ce exerts a potent purifying influence on Fe and Si impurities within the aluminium matrix, resulting in the creation of Al–Fe-Si-Ce compounds rather than a solid solution [18, 19]. After heat treatment, most atoms of solid solutions in Al-La and Al-Ce alloys can completely precipitate from the aluminium matrix [15]. 0.3 mass % La-rich RE mixtures has an optimal effect on the microstructure and mechanical properties of an Al-2 mass % Fe alloy. The modification with rare earths (RE) refined the α-Al grains, causing a separation of the eutectic and the emergence of Al_xFe_y phases in the form of discontinuous networks, flakes, and particles. Nevertheless, introducing 0.4 mass % RE resulted in the clustering of Al-Ce particles, negatively impacting the mechanical properties of the alloys [20]. Through the dissolution of elemental Ce in the Al_xFe_y phase and subsequent homogeneous annealing, the claw-like Al_xFe_y phases underwent a transformation into short flakes and particles. These transformed elements were uniformly dispersed in the matrix through rolling processes [3].

Hence, various approaches have been employed to mitigate the adverse impacts of Al–Fe intermetallic phases by diminishing their size and altering their morphology and distribution. Nevertheless, a detailed investigation into the influence of rare earth (RE) elements on solidification and phase formation in Al–Fe alloys has not been extensively explored. In this study, alloys from the Al–Fe system were prepared in the laboratory from pure raw materials. To specify the solidification and phase formation in the experimental alloys, different amounts of RE—cerium and/or lanthanum—were added. Since solidification is never completely in equilibrium, a number of metastable intermetallic Fe phases can be observed in the microstructure. We have focused on the formation temperature and shape of the intermetallic phases in the presence of La and/or Ce, as they can increase the corrosion resistance and mechanical properties, as well as forming properties of aluminium alloys.

Materials and methods

The addition of rare earths (Ce and/or La) to the Al-1.4 mass % Fe alloy was planned using simulations in the Thermo-Calc 2022b program with a TCAL6 database (Thermo-Calc Software AB, Stockholm, Sweden). Scheil simulations were performed for 0.15 mass % La, 0.15 mass % Ce, and simultaneous 0.1 mass % Ce and 0.1 mass % La additions to the Al-1.4 mass % Fe alloy to predict the influence of RE elements on the phase formation and the formation temperature of the relevant phases. The number of equilibrium phases at room temperature was also calculated.

Al-1.4 mass % Fe–x mass % Ce/La alloys (x=0.15 mass % Ce or La and 0.2 mass % Ce and La) were prepared from pure raw metals (Al-99.99%, Fe-99.99%, Ce-99.99%, and La-99.9%) in an induction furnace and a steel crucible coated with BN-cast coating and poured into a Cronning measuring cell equipped with a type K thermocouple, whereas the cooling curves (temperature vs. time) were

Table 1 Chemical composition in mass % and designations of experimental alloys

Sample	Fe	Cu	Si	Mn	Mg	Ce	La	Al
K0	1.14	0.0009	0.0062	0.0013	0.0008	< 0.001	< 0.001	Rest
K1	1.43	0.0012	0.0081	0.0023	0.0008	< 0.001	0.139	Rest
K2	1.38	0.0011	0.0087	0.0058	0.0008	0.147	< 0.001	Rest
K3	1.43	0.0012	0.0088	0.0075	0.0009	0.0708	0.0909	Rest

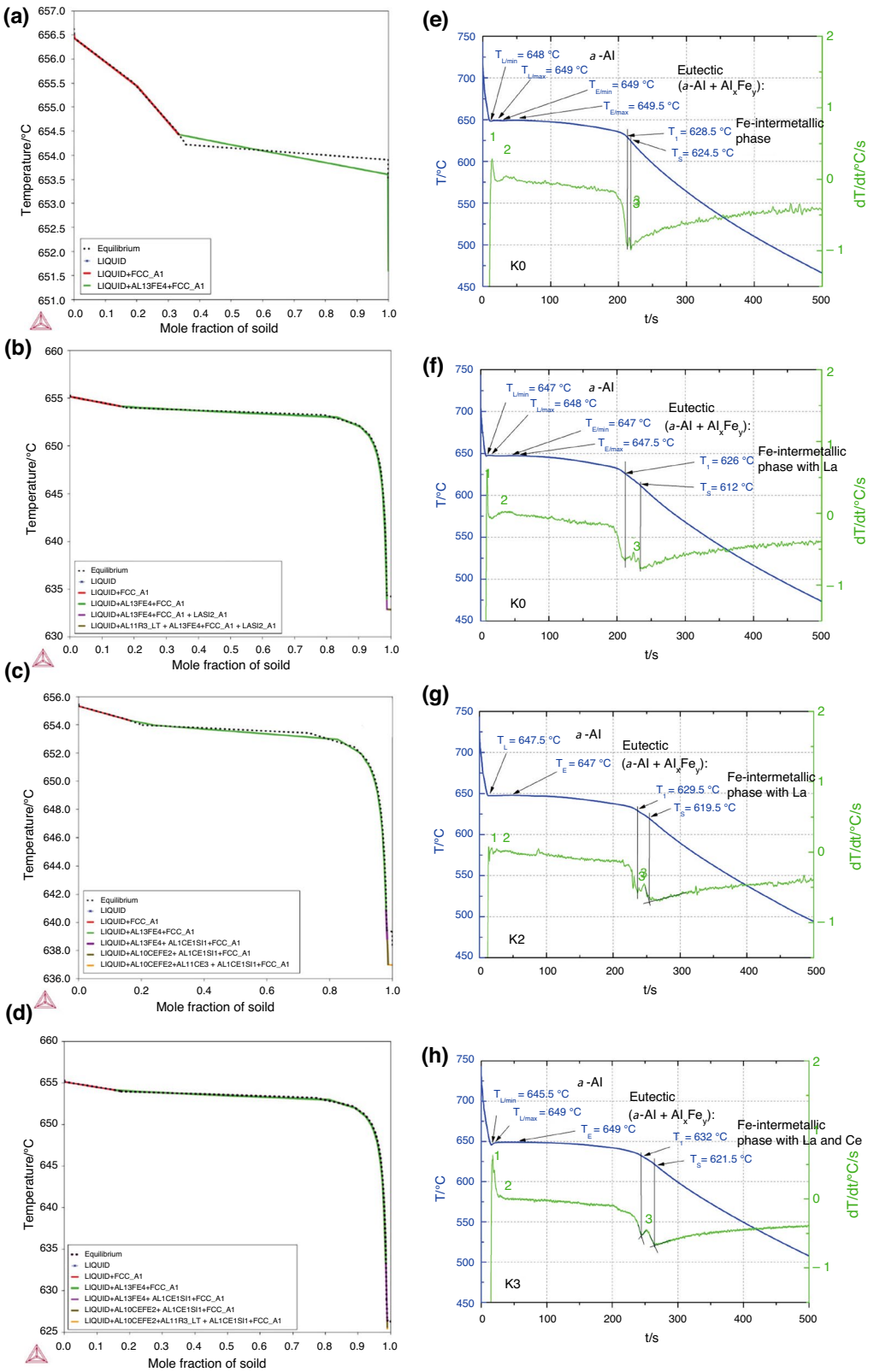

Fig. 1 Mass fractions of all solids formed during solidification of the alloys studied: K0 (**a**), K1 (**b**), K2 (**c**) and K3 (**d**). The simulation is based on the Scheil model. Langside are presented solidification curves and its first derivatives for alloys K0—reference Al-1.4Fe (**e**), K1 (**f**), K2 (**g**) and K3 (**h**). Peak 1 on the derivative curve corresponds to the α-Al dendrite, peak 2 to the Al–Fe eutectic and peak 3 to the Fe-containing intermetallic phase

Table 2 Temperatures of phase solidification in nonequilibrium in °C, calculated according to the Scheil model

Phase/Sample	K0	K1	K2	K3
α_{Al}	656.5	655.5	655.5	655.5
$Al_{13}Fe_4$	654.5	654	654.5	654
AL1CE1SI1 (AlCeSi)			641	633.5
AL10CEFE2 ($Al_{10}Ce_3Fe_2$)			639	626.5
AL11CE3 ($Al_{11}Ce_3$)			637	
LASI2_A1 ($LaSi_2$)		635		
AL11R3 ($Al_{11}La_3$)		633		625.5
T_S	651.5	632.5	636.5	625.0
$\Delta T_{solidification}$	5	23	19	30.5

recorded. The melting and casting process was as follows: First, pure Al and Fe were melted, whereas the chemical composition was analysed to make sure that aimed Al-1.4 mass. % Fe alloy was reached. Further, when the temperature of the alloy (Al–Fe) reached 750 °C in the furnace, the RE additives were added and mixed, and after 10 min, the alloy was poured into the Cronning measurement cell, with the temperature being tracked over time. The cooling rate in the Cronning measuring cell amounts approximately 7 K/s. The temperature vs. time curves were plotted and the characteristic solidification temperature of the test alloys was marked. The chemical compositions of the test alloys are listed in Table 1.

To assess the validity of the simulation and cooling curve outcomes, all test alloys underwent analysis through both differential scanning calorimetry (DSC) and microstructure examination. DSC tests were conducted using a DSC 404 F1 Pegasus instrument from the NETZSCH Group, Selb, Germany. The tests involved samples from the Cronning measuring cell centre placed in an empty reference corundum pan, with scans performed in a dynamic argon atmosphere. The samples were heated to 720 °C at a rate of 10 K min^{-1}, held at this temperature for 10 min, and subsequently cooled to room temperature at the same rate of 10 K min^{-1}. The characteristic melting and solidification temperatures were deduced from the recorded DSC curves.

Samples from the Cronning measuring cell were also subjected to standard metallographic preparation. Microscopic examinations were carried out using an Olympus BX61 microscope equipped with a DP70 camera (Olympus Europa SE and Co. KG, Hamburg, Germany) at magnifications of 50 and 500.

Results and discussion

According to the calculations of TC using the Scheil module (Fig. 1), the traces of Ce and La in the Al-1.4Fe alloy shift the liquidus temperature, the temperature of the eutectic (α-Al + $Al_{13}Fe_4$) solidification and the solidification of the Fe-bearing intermetallic phases to a lower temperature. The temperatures presented are listed in Table 2. The inclusion of La can refine the α-Al grain through three mechanisms: (1) promoting the formation of nucleation sites (2) restricting the growth of α-Al grains and (3) decreasing the wetting angle (θ) between the nucleation sites and the α-Al nucleus. This is substantiated by thermodynamic data and experimental findings detailed in earlier literature [13, 21]. Some authors also reported that the traces of Ce and/or La may act as surfactants and thus refine the α-Al grains, but

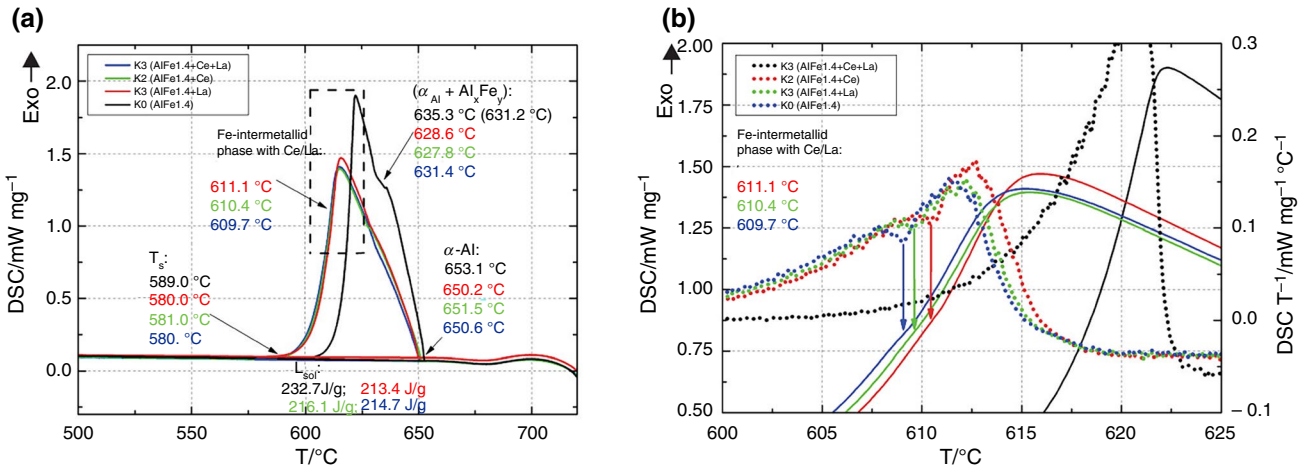

Fig. 2 Cooling DSC curves of experimental alloys (**a**): K0 (black), K1 (red), K2 (green), and K3 (blue), with the characteristic temperatures, phases and enthalpies plotted, and the magnified range of the solidification temperature of the Fe-containing intermetallic phases and their corresponding derivatives (**b**)

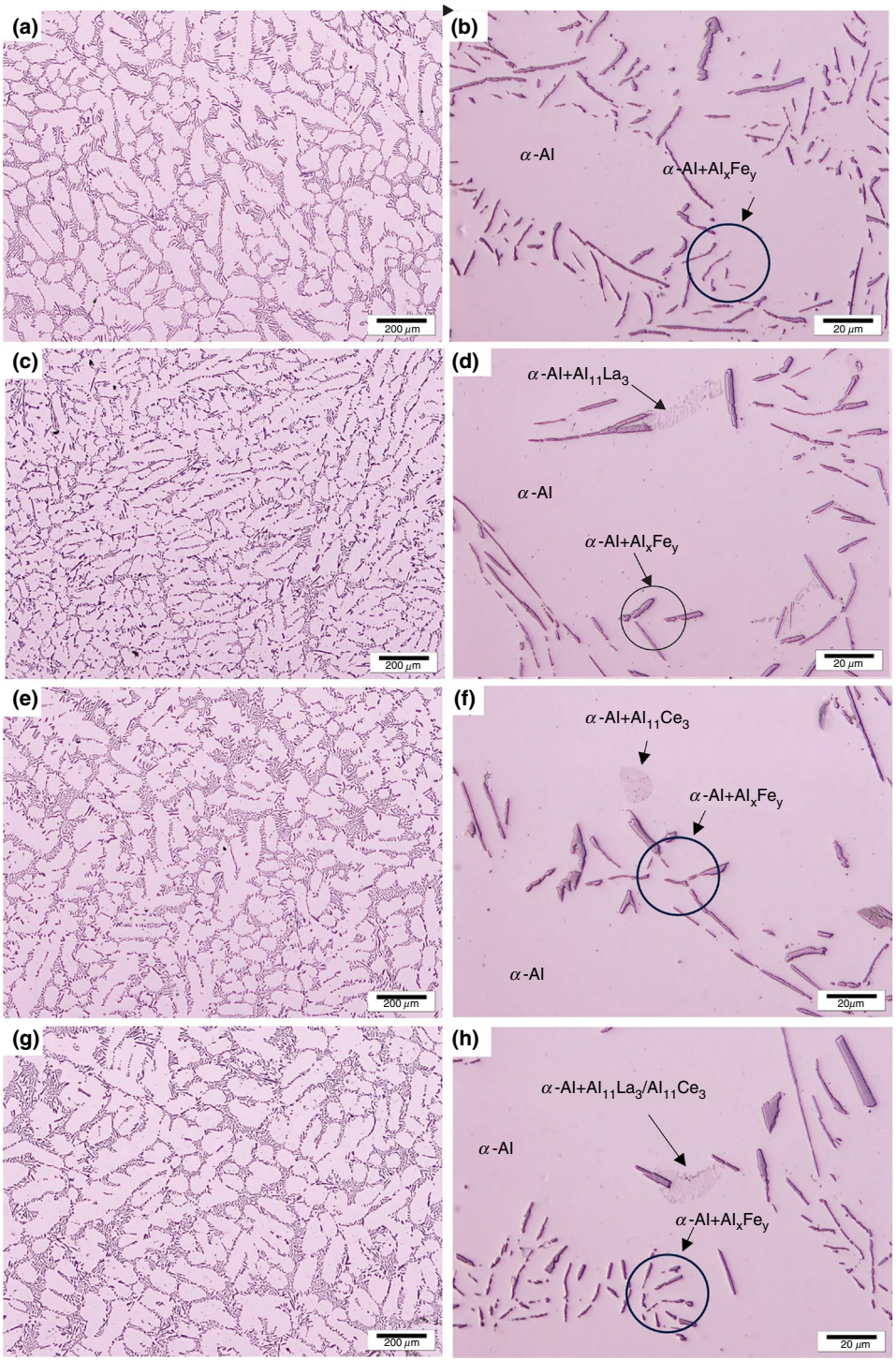

Fig. 3 Microstructure of investigated samples at magnification 50 and 500: sample K0 (**a**, **b**), sample K1 (**c**, **d**), sample K2 (**e**, **f**) and sample K3 (**g**, **h**)

our calculations could not confirm this. This could also be due to a lower Fe content in sample K0.

According to Jiang et al. [10], La modifies the $Al_{13}Fe_4$ by adsorbing the La element on the growth edges of the $Al_{13}Fe_4$, resulting in a modified morphology of the $Al_{13}Fe_4$ eutectic phase with an acicular or rod-like shape, which plays a crucial role in the strength and ductility of EN AW 8xxx alloys [22]. With the addition of about 0.139 mass % La, the La-bearing phase $Al_{11}La_3$ is expected to form after the main eutectic at 633 °C. According to our calculations, Ce forms phases with Al and Si or Fe in the Al-1.4% Fe alloy, with the latter expected in higher concentrations. At this ratio (0.147 mass % Ce), Ce can also form an $Al_{11}Ce_3$ phase in the microstructure. With small additions of Ce

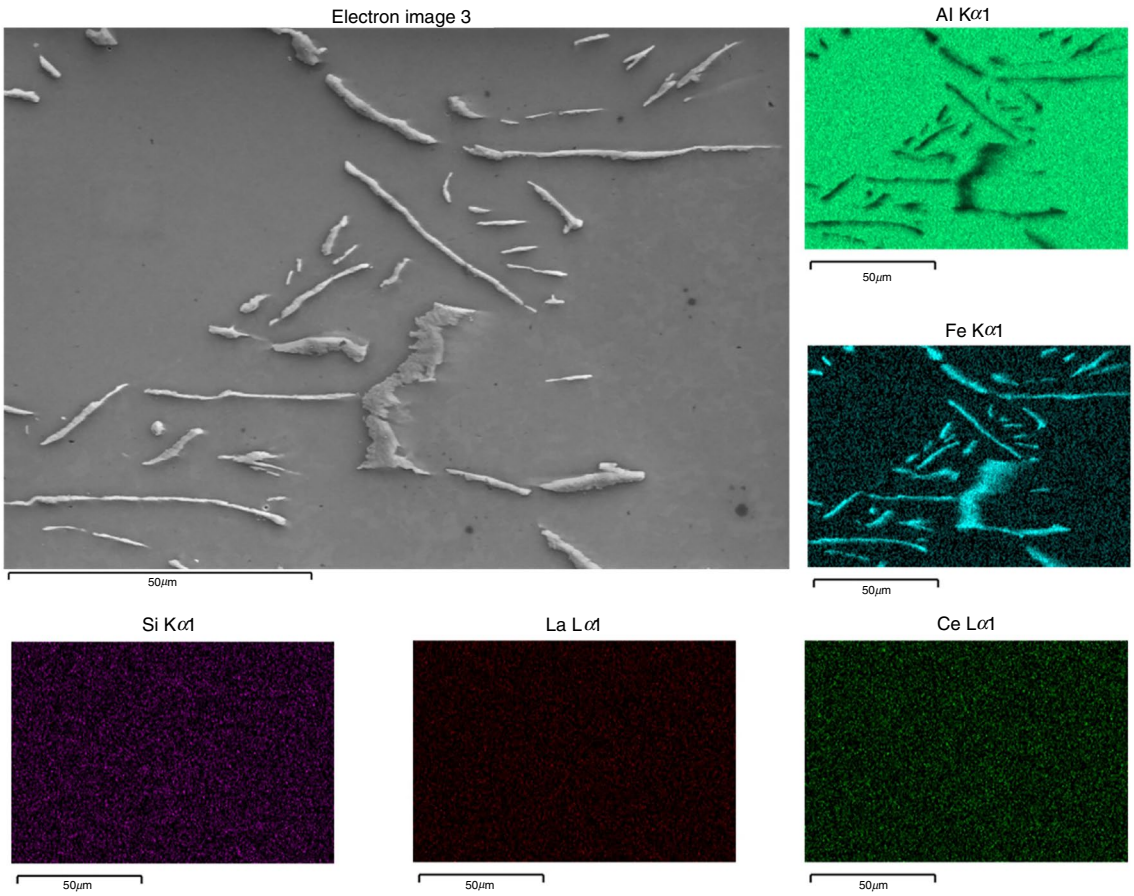

Fig. 4 SEM image and EDS mapping of the reference alloy K0 (Al-1.4Fe)

and/or La, the freezing range is extended and calculated as the temperature difference between liquidus and solidus temperatures (Table 2).

Figure 1e illustrates the cooling curve of the reference alloy, designated as sample K0. Figure 1e-h also depicts the corresponding first derivative curves, which play a crucial role in unveiling subtle changes in the cooling curve. For the reference alloy, the derivative curves exhibit three distinct peaks, each indicative of the formation of a new phase. The initial phase, α-Al, appeared at 648 °C with a $T_{L/min}$ (evidenced by the first deflection on the cooling curve), coinciding with recalescence. This was followed by the formation of the eutectic phase Al–Fe at 649 °C (maximum at the derivative curve marked as peak 2). Due to a high cooling rate, the nonequilibrium solidification of this eutectic occurred at a temperature 1 °C higher than α-Al. As cooling progressed, the remaining liquid solidified in the form of a Fe-containing intermetallic eutectic phase at 628.5 °C (starting point at the derivative curve marked as peak 3). The cooling and derivative curves of the La-modified alloy are shown in Fig. 1f. All solidification temperatures are slightly lower when La is added to the Al-1.4Fe alloy. The solidification temperature range of peak 3 is wider, indicating changes in the solidification of nonequilibrium Fe-bearing intermetallic phases. At this temperature, La could form individual $Al_{11}La_3$ at 0.14 mass % La content in alloy K1. The cooling and derivative curves of the Ce-modified alloy are shown in Fig. 1g. The solidification range of the Fe-intermetallic alloy is also wider in this case, indicating changes in the solidification phases. Ce is incorporated into the Fe-bearing intermetallic phase or even forms its own phases, namely $Al_{11}Ce_3$ or/and AlFeCe and/or AlSiCe, according to our calculations and literature data [9]. The solidification process is similar to that of the reference alloy, but at slightly lower temperatures, indicating a change in the forming phases due to the Ce addition. As shown in Fig. 1h, the Ce- and La-modified alloy began to solidify at a lower temperature than the Ce- and La-free alloy. The first derivative of the cooling curve also shows a wider temperature range for solidification in this case.

For both the base and modified alloys under investigation, the freezing range was computed as the difference between the liquidus and solidus temperatures. The liquidus

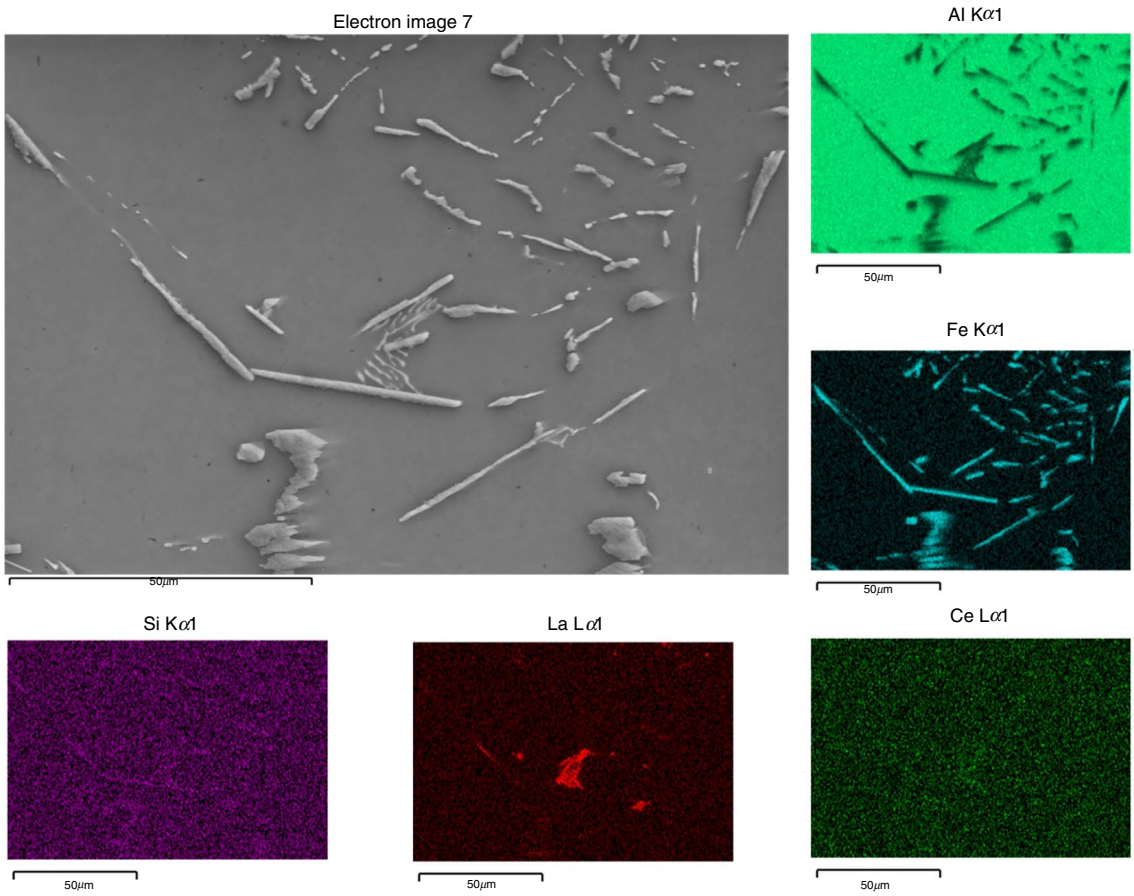

Fig. 5 SEM image and EDS mapping of the K1 alloy with La

temperature was determined by considering the minimum liquidus temperature of the α-Al phase, while the solidus temperature was ascertained based on the final deviation from the derivative curve. In the case of the reference alloy, the liquidus and solidus temperatures were 648 °C and 624.5 °C, respectively. Following the addition of La, the liquidus temperature decreased to 647 °C, and the solidus temperature dropped to 612 °C. Similar trends were observed for alloys K2 and K3. It can be inferred that the incorporation of the rare earth element Ce and/or La resulted in an expansion of the freezing range. Generally, the fluidity of a metal is inversely proportional to its freezing range. Hence, based on these findings, the casting process tends to become more susceptible to solidification-related defects [23].

Both analysis results, simulated by TC (Fig. 1a-d) and experimental solidification curve (Fig. 1e-h) give matching results. The addition of Ce and/or La to Al-1.4Fe alloy lowers liquidus temperature and increases the freezing range.

Figure 2 shows the DSC results for the alloys studied without and with various RE additions. The results show that at a cooling rate of 10 K min^{-1}, the α-Al solidifies at 653.1 °C in the RE-free alloy and decreases to 650.2 °C, 651.5 °C and 650.6 °C when 0.139 mass % La, 0.147 mass % Ce, and 0.0708 mass % La and 0.0909 mass % Ce are added to the Al-1.4 mass % Fe alloy, respectively. The decrease in solidification temperature is also observed in the eutectic solidification of Al_xFe_y phase, indicating that these RE elements affect the nucleation behaviour of Al_xFe_y phase. Solidification of Fe-containing intermetallic phases was almost undetectable in the RE-free alloy, but clearly visible in all other alloys containing RE elements (Fig. 2b). From the DSC results, the freezing range was again calculated as the difference between liquidus and solidus temperatures, and again, there was an increase in the freezing range when RE elements were added to the Al-1.4Fe alloy. All results, TC simulations, solidification curve analysis and DSC analysis give matching results. The solidification enthalpies are significantly lower when RE elements are added to the alloy.

Figure 3 shows the microstructure of Al-1.4Fe alloys in the as-cast state with different RE. The microstructure in

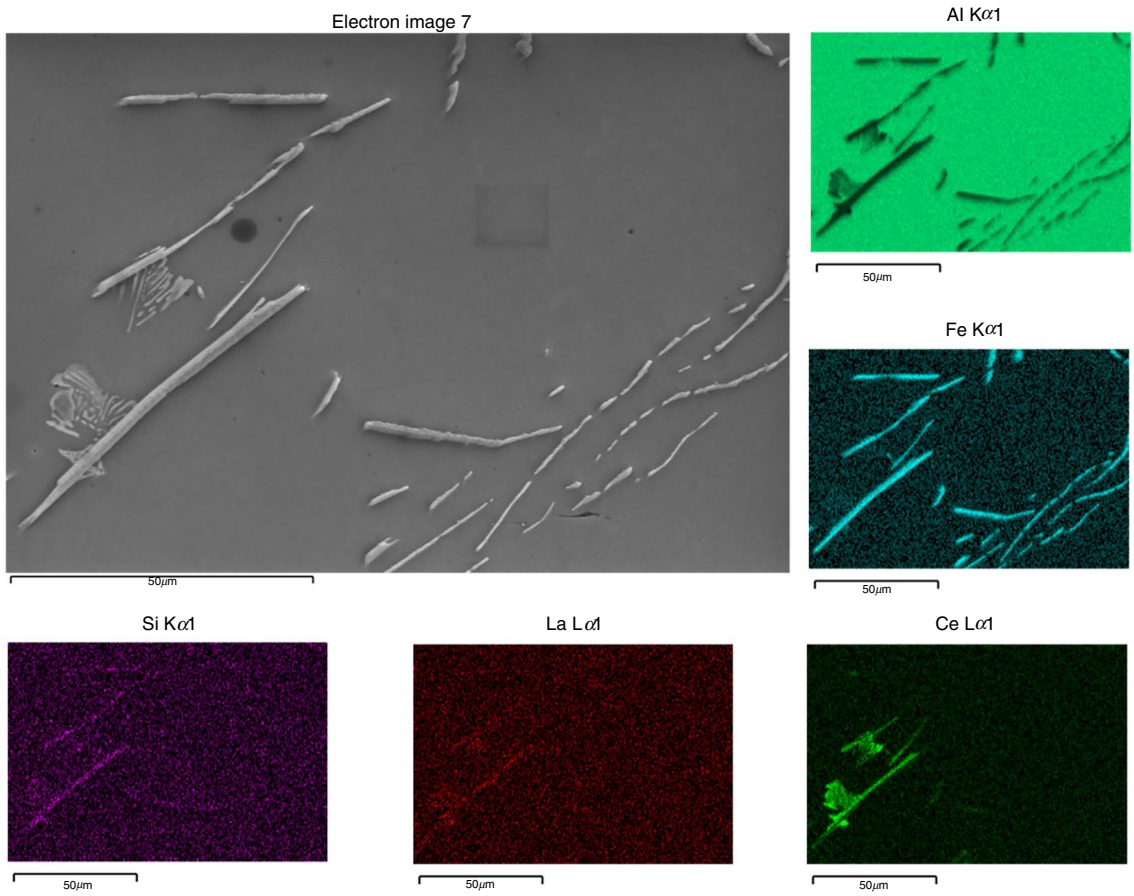

Fig. 6 SEM image and EDS mapping of the K2 alloy with Ce

Fig. 3 is a typical hypoeutectic microstructure composed of the primary α-Al and the eutectic (α-Al + Al_xFe_y). The effect of dendritic microstructure refinement of the primary α-Al phases of the as-cast alloy with the addition of RE can be observed, with La showing the most expressive result. This is consistent with the results reported in [8]. The effect of the RE additions shows no obvious differences in the morphology of the eutectic Al_xFe_y phase. The Al_xFe_y phase observed in the microstructure consists of a stable Al_3Fe phase and a mostly metastable Al_6Fe phase, which can be attributed to a high cooling rate of the samples. The Al_3Fe phase consists of coarser lamellae, while the Al_6Fe phase consists of fine fibres grouped in cellular structures of uniformly oriented fibres [24].

When La and/or Ce are added, these elements are expected to form phases with Al and Fe. When La was added in samples K1 and K3, Al–La and Al–Fe–La bearing phases occurred in small amounts, and they formed always near each other. Without EDS maps (Figs. 4–7), the Al–Fe–La bearing phase is difficult to visually define as its morphology and colour are the same as Al_xFe_y eutectic phase. In samples K2 (Fig. 3e, f) and K3 (Fig. 3g, h), an (α-Al + $Al_{11}Ce_3$) eutectic formed, which was unevenly distributed in the alloy. To confirm these claims, EDS maps are presented (Figs. 6 and 7). When Ce were added in samples K2 and K3, Al_8Fe_2Ce did occur in small amounts, and, also in this case, was always present near the $Al_{11}Ce_3$ containing eutectic. As a result of the formation of these phases together in the last solidification zone, the last peak is wider on the derivative cooling curve (Figs. 1f–h), and desorption can be detected on the derivative DSC curve (Fig. 2b). In the case of sample K3, La and Ce bonded together with Al or Al and Fe, forming Al–Ce–La and Al–Fe–Ce–La bearing phases, respectively. Calculations according to the Scheil (Fig. 1a-d and Table 2) also predict the solidification of Si–La bearing phases in the presence of La, but they were not detected in the analysed microstructure of the investigated samples, as the content of Si is very low.

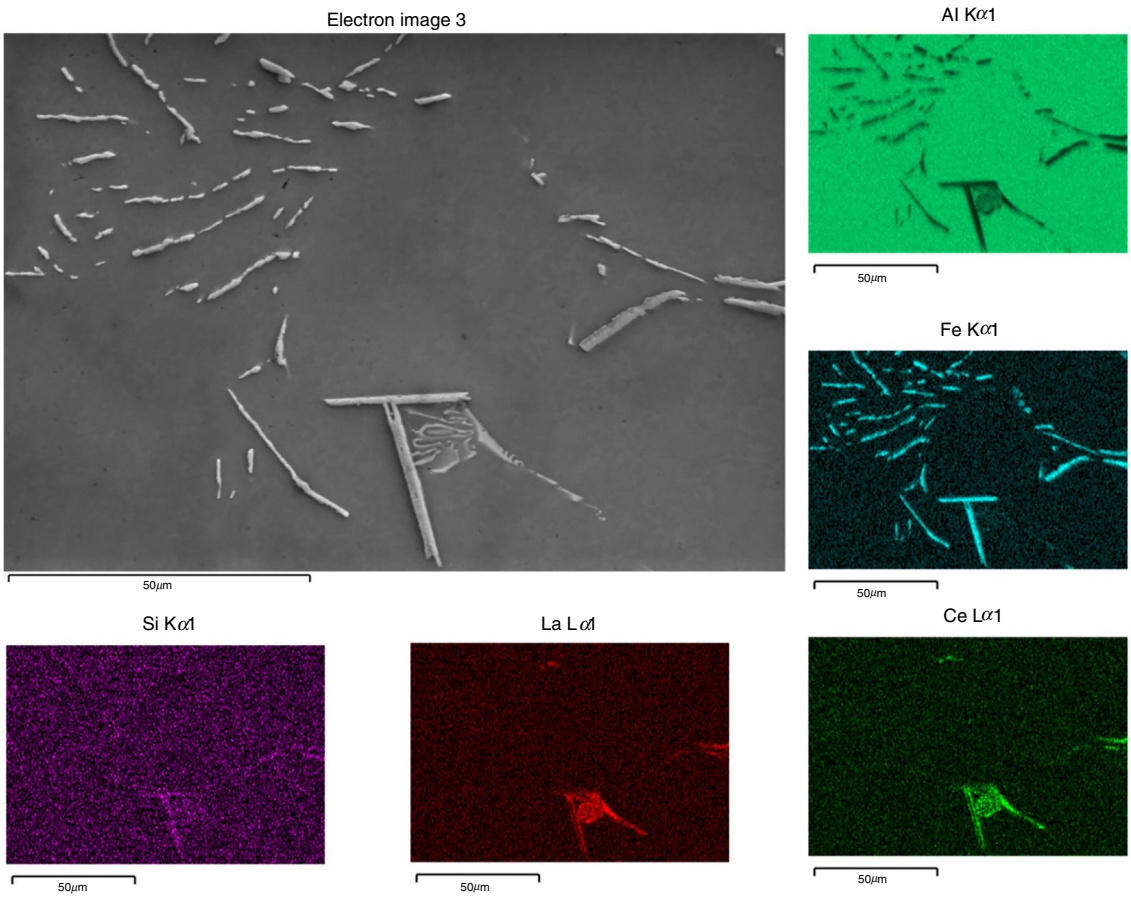

Fig. 7 SEM image and EDS mapping of the K3 alloy with La and Ce

Conclusions

Alterations in the temperature at which a specific phase initiates are typically interpreted as indicative of a modification in that phase due to the introduced element. Thermal analysis of the solidification behaviour of the reference alloy unveiled three reactions corresponding to the formation of α-Al, a eutectic (α-Al + Al_xFe_y) and Fe-intermetallics with Ce and La, respectively. The findings demonstrated analogous reactions for the Ce and/or La-modified alloy, occurred at slightly lower temperatures, suggesting a shift in the phases being formed due to the incorporation of Ce and/or La. The microstructure of the test alloys was typically hypoeutectic in all cases. The grain refining effect of the primary α-Al grains of the as-cast alloy was observed by the addition of RE, while La showed the strongest effect. The effects of the additions of RE showed no obvious differences in the morphology of the eutectic Al_xFe_y. When La and/or Ce are added, these elements are expected to form phases with Al and Fe, whereas the morphology does not change. In some cases, Ce and La are incorporated into Al–Fe eutectic phase. When Ce and/or La were added, (α-Al + $Al_{11}Ce_3$) and (α-Al + $Al_{11}La_3$) eutectics were formed, respectively, while Fe was not detected in these eutectics.

Acknowledgements We gratefully acknowledge the financial support of the Slovenian Research and Innovation Agency (ARIS) for funding under program grant P2-0344(B).

Author contributions M.V. was involved in conceptualization, methodology, investigation, validation and writing—reviewing and editing; K.O. was responsible for investigation, validation and writing—reviewing and editing; J.M. contributed to writing—reviewing and editing; and M.S. took part in investigation and writing—reviewing and editing. All authors have read and agreed to the published version of the manuscript.

Funding This research was funded by the Slovenian Research and Innovation Agency (ARIS) under the program Advanced Metallurgy, grant number P2-0344(B).

Declarations

Conflicts of interest The authors declare no conflict of interest.

References

1. Van Horn KR. Aluminium Properties, physical metallurgy and phase diagrams Metals park. Am Soc Met. 1967;1:425.
2. Sidney L. Aluminium alloys—new trends in fabrication and applications. New York: scitus academics LLC. 2017 370
3. Shi ZM, Gao K, Shi YT, Wang Y. Microstructure and mechanical properties of rare-earth-modified Al−1Fe binary alloys. Mater Sci Eng. 2015;632:62–71.
4. Li H, Wang X, Zhu X, Duan X, Pan A. Composition modulation in one-dimensional and two-dimensional chalcogenide semiconductor nanostructures. Chem Soc Rev. 2018;47:7504–21.
5. Li H, Wu X, Liu H, Zheng B, Zhang Q, Zhu X, Wei Z, Zhuang X, Zhou H, Tang W, Duan X, Pan A. Composition-modulated two-dimensional semiconductor lateral heterostructures via layer-selected atomic substitution. ACS Nano. 2017;11:961–7.
6. Li H, Liu H, Zhou L, Wu X, Pan Y, Ji W, Zheng B, Zhang Q, Zhuang X, Zhu X, Wang X, DuanX PA. Strain-tuning atomic substitution in two-dimensional atomic crystals. ACS Nano. 2018;12:4853–60.
7. Moldovan P, Popescu G, Miculescu F. Microscopic study regarding the microstructure evolution of the 8006 alloy in the plastic deformation process. J Mater Process Technol. 2004;153:408–15.
8. Liang YH, Shi ZM, Li GW, Zhang RY, Li M. Effects of rare earth modification on microstructure refinement and mechanical properties of Al-2wt%Fe alloys. Mater Res Express. 2019;6:106504.
9. Mahmoud MG, Mosleh AO, Mohamed MS, El-Moayed MH, Khalifa W, Pozdniakov AV, Salem S. The impact of Ce-containing precipitates on the solidification behavior, microstructure, and mechanical properties of Al-6063. J Alloy Compd. 2023;948:169805.
10. Jiang H, Li S, Zhang L, He J, Zheng Q, Song Y, Li Y, Zhao J. The influence of rare earth element lanthanum on the microstructures and properties of as-cast 8176 (Al-0.5Fe) aluminum alloy. J Alloys Compd. 2021;59:157804.
11. Zhang Sb SuY, Gong WG. Effects of rare earth elements on microstructure and tensile properties of Al-Si-Cu alloy at 250 °C. China Foundry. 2021;18:474–80.
12. Ibrahim MF, Abdelaziz MH, Samuel AM. Effect of rare earth metals on the mechanical properties and fractography of Al–Si-based alloys. Inter Metalcast. 2020;14:108–24.
13. Tsai YC, Chou CY, Lee SL, Lin CK, Lin JC, Lim SW. Effect of trace La addition on the microstructures and mechanical properties of A356 (Al–7Si–0.35Mg) aluminum alloys. J Alloys Compd. 2009;487:157–62.
14. Zhang Y, Wei F, Mao J, Niu G. The difference of La and Ce as additives of electrical conductivity aluminum alloys. Mater Charact. 2019;158:109963.
15. He Y, Liu J, Qiu S, Deng Z, Zhang J, Shen Y. Microstructure evolution and mechanical properties of Al-La alloys with varying La contents. Mater Sci Eng. 2017;701:134–42.
16. Jiang W, Fan Z, Dai Y, Li C. Effects of rare earth elements addition on microstructures, tensile properties and fractography of A357 alloy. Mater Sci Eng A. 2014;597:237–44.
17. Alkahtani SA, Elgallad EM, Tash MM, Samuel AM, Samuel FH. Effect of rare earth metals on the microstructure of Al-Si based alloys. Materials. 2016;9(45):1–13.
18. Pengfei L, Zhigang W, Yunli W, Xizhu G, Zaiyun W, Zhiqiang L. Effect of cerium on mechanical performance and electrical conductivity of aluminum rod for electrical purpose. J Rare Earths. 2006;24:355–7.
19. Ahmad R, Asmael MBA. Influence of cerium on microstructure and solidification of eutectic Al–Si piston alloy. Mater Manuf Processes. 2016;31:1948–57.
20. Luo SX, Shi ZM, Li NY, LinYM LYH, Zeng YD. Crystallization inhibition and microstructure refinement of Al-5Fe alloys by addition of rare earth elements. J Alloys Compd. 2019;789:90–9.
21. Raghavan V. Al-Fe-La (Aluminum-Iron-Lanthanum). J Phase Equilib. 2001;22:566–7.
22. Zheng QJ, Zhang LL, Jiang HX, Zhao JZ, He J. Effect mechanisms of microalloying element La on microstructure and mechanical properties of hypoeutectic Al-Si alloys. J Mater Sci Technol. 2020;47:142–51.
23. Ravi KR, Pillai RM, Amaranathan KR, Pai BC, Chakraborty M. Fluidity of aluminum alloys and composites: a review. J Alloy Compd. 2008;456:201–10.
24. Cubero-Sesin JM, Watanabe M, Arita M, Horita Z. Aging and precipitation behavior in supersaturated Al-2%Fe alloy produced by high-pressure torsion. Mater Sci Forum. 2014;794–796:766–71.